A Wideband Omnidirectional Horizontally Polarized Traveling-Wave Antenna Based on Half-Mode Substrate Integrated Waveguide

Nghia Nguyen-Trong, *Student Member, IEEE*, Thomas Kaufmann, *Member, IEEE*, and Christophe Fumeaux, *Senior Member, IEEE*

***Abstract*—A traveling-wave antenna based on a tapered half-mode substrate integrated waveguide is introduced in this letter. It uses a direct transition from a coaxial connector and radiates from the open side of the waveguide. The antenna exhibits a wide bandwidth, an omnidirectional radiation pattern, and horizontal polarization and can be integrated into metallic structures. The physical principle and design guidelines are summarized. A prototype of the proposed antenna has been realized and demonstrated a wide measured bandwidth extending from 6.7 to 16 GHz, with radiation characteristics corresponding very well with simulations.**

***Index Terms*—Half-mode substrate integrated waveguide (HMSIW), omnidirectional radiation pattern, wideband antenna.**

I. Introduction

SINCE its introduction in 2006 [1], the half-mode substrate integrated waveguide (HMSIW) has been intensively investigated for many applications, especially due to its benefits at higher microwave frequencies. While preserving the advantages of a substrate integrated waveguide (SIW) such as low loss, small size, and ease of integration with planar circuits [2], its geometrical dimension is reduced by half compared to that of an SIW. Thus, the HMSIW is easy to fabricate and suitable for millimeter-wave (mm-wave) applications. Several HMSIW antenna applications have been introduced previously based on periodic perturbations, such as a leaky-wave antenna (LWA) [3] or a transverse slot-array antenna [4]. Furthermore, based on the radiation loss of the HMSIW close to cutoff frequency, a different concept of uniform LWA has been introduced in [5]. However, as this antenna is designed to work at a specific frequency, i.e., close to cutoff frequency, its bandwidth is accordingly restricted. In all cases, as the power radiates from an array of slots or a long aperture, the obtained radiation patterns are highly directive.

The antenna proposed in this letter is designed based on the same concept, i.e., high radiation loss of the HMSIW close to cutoff but with a different approach. The cutoff frequency is varied along the length of the antenna by tapering the HMSIW width as shown in Fig. 1. The wave is guided along the HMSIW structure until it reaches the position where the cutoff frequency is close to the operating frequency, i.e., where the radiation losses from the open side of the guide become significant and the antenna starts to radiate intensively. Since the antenna is built from an HMSIW structure, it has a thin body that can be completely embedded in planar structures (Fig. 1). This relatively simple geometry can be manufactured at a low cost, as it only requires standard technologies in the fabrication of planar circuits and SIWs. Yet, the antenna achieves omnidirectional horizontally polarized radiation characteristics over a very wide fractional bandwidth (over 80% demonstrated here).

Fig. 1. Manufactured HMSIW traveling-wave antennas after connector assembly. The open sides of the HMSIWs are toward the bottom. Realization with solid copper walls on top, equivalent structure with copper via holes at the bottom.

Despite a relatively large length, this antenna exhibits small profile and width, which makes it suitable for integration into metallic structures such as poles, masts, or incorporated into an aircraft fuselage as a load-bearing antenna. This antenna can find applications in wireless communication systems requiring omnidirectional radiation with horizontal polarization, or as diversity counterpart to standard monopole antennas. Reduced size can also be tailored for the intended application, as a tradeoff exists between the length of the antenna and the operation bandwidth.

This letter is structured as follows. First, the feeding mechanism realized through a coaxial-to-HMSIW transition is summarized. Then, the physical principle and design guidelines are explained in detail. Finally, simulation and experimental results are compared to verify the characteristics of the antenna.

II. Coaxial-to-HMSIW Transition

An appropriate feeding section for this antenna is crucial to achieve satisfactory polarization purity. To this end, the proposed antenna features a direct feed from a coaxial SMA connector. The coaxial cable is connected perpendicularly to the HMSIW through a capacitive gap. This technique is adapted toward HMSIW from previous realizations of feeding to SIW structures [6], [7].

The substrate material selected for antenna fabrication is Rogers Ultralam 2000 with relative permittivity of $\varepsilon_{\mathrm{r}} = 2.5$

Manuscript received January 10, 2013; revised April 15, 2013; accepted May 09, 2013. Date of publication May 16, 2013; date of current version May 30, 2013. The work of C. Fumeaux was supported by the Australian Research Council (FT100100585).

The authors are with the University of Adelaide, Adelaide, SA 5005, Australia (e-mail: nghia.nguyentrong@student.adelaide.edu.au; thomas.kaufmann@adelaide.edu.au; cfumeaux@eleceng.adelaide.edu.au).

Color versions of one or more of the figures in this letter are available online at http://ieeexplore.ieee.org.

Digital Object Identifier 10.1109/LAWP.2013.2263492

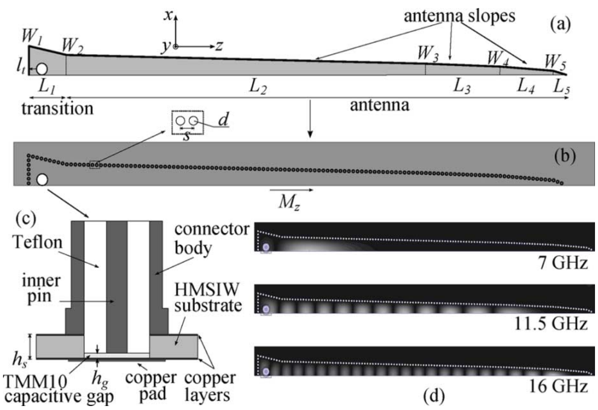

Fig. 2. (not to scale) (a) PEC-wall antenna configurations. The metal walls are shown as thicker lines. (b) Via-wall antenna constructed from PEC-wall antenna. (c) Coaxial–HMSIW transition. (d) Electric field plots at three chosen frequencies.

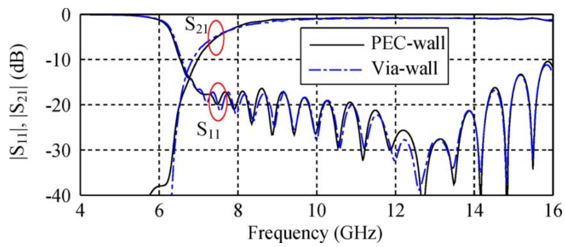

Fig. 3. Scattering parameters for an arrangement of two back-to-back coaxial–HMSIW transitions, with an HMSIW of length 120 mm in between.

and thickness of $h_s = 1.524$ mm (60 mil). The transition and its dimensions optimized by ANSYS HFSS are shown in Fig. 2(a) with $W_1 = 10$ mm, $W_2 = 7$ mm, $L_1 = 14$ mm, and $l_t = 4.4$ mm. Instead of the classical HMSIW structure with an extended ground plane and substrate extending past the open side of the guide, the substrate of the antenna is truncated at the aperture toward the negative x-direction to obtain omnidirectional radiation patterns.

For a wideband matching to the HMSIW, the imaginary part of the input impedances is decreased through a capacitive gap in the arrangement shown in the side view [Fig. 2(c)]. This gap is accurately realized using a thin layer of Rogers TMM10 material (relative permittivity of 9.2) with thickness of $h_g = 0.381$ mm (15 mil). This is a relatively large thickness that corresponds to a quarter of the substrate thickness and simplifies the manufacturing process of the transition. Generally, emphasis has be placed to achieve a final design that is both robust to tolerances and simple to manufacture. The transition is first designed with a simplified perfect electric conducting (PEC) wall for faster simulation times and numerically verified using metal vias in a final step. The S-parameters for two back-to-back transitions with an HMSIW of 120 mm length in between are shown in Fig. 3. The simulated reflection coefficients $|S_{11}|$ are below -15 dB between 7 and 15 GHz, and the insertion loss decreases to 1 dB above 9.5 GHz.

III. Antenna Principle and Design Process

In this section, the operation principle of the antenna is qualitatively explained first. Then, a proposed design process using simulation software is described in detail followed by the manufacture procedure of the antenna and its coaxial transition.

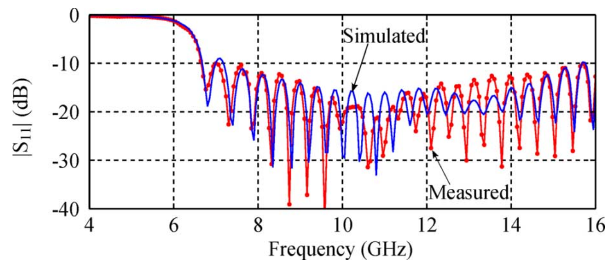

Fig. 4. Simulation and measurement of reflection coefficient for via-wall antenna.

A. Operation Principle

The antenna concept is based on the radiation-loss characteristic of the HMSIW. When the operating frequency is close to the cutoff frequency, the radiation losses of the HMSIW become extremely high [8]. At this stage, the open side of the HMSIW can be considered as a thin open aperture. The proposed antenna exploits this radiation-loss mechanism by tapering the HMSIW width, i.e., by progressively increasing the cutoff frequency along its length. This feature of varying cutoff frequency supports the wideband characteristics of the radiator. In other words, the guided wave will travel along the HMSIW until it reaches the position where the corresponding cutoff frequency is close to the operating frequency, as illustrated in Fig. 2(d). The HMSIW open side starts then to act as a short magnetic dipole antenna with current distribution of [8]

$$\vec{M}_z = -Ak_x \sin(k_x w) e^{-jk_z z} \vec{a}_z \tag{1}$$

at the aperture. Due to the tapering effect, the wavenumbers k_x, k_z and the guide width w are functions of the position z. In short, each frequency component will be radiated from a small portion of the antenna length at different positions along the open side of the HMSIW.

B. Design Process

The simulation of the antenna with the HMSIW side walls made as a row of vias is very time-consuming. Therefore, the design process starts with the side wall realized as PEC wall with an equivalent width ([9, Eq. (9)]). The main design feature is the rate at which the HMSIW is tapered. The simulations show a tradeoff between antenna directivity and reflection coefficient. A steeper slope results in a higher reflection coefficient but a smaller directivity. This can be understood intuitively as, in this case, the tapering is faster, while the antenna only radiates from a smaller aperture.

The radiation mechanism of the structure also suggests that the tapering can become more aggressive toward the antenna thin end to decrease the effective aperture length where the higher-frequency components are radiated. Therefore, four different tapering slopes have been introduced along the antenna and optimized using HFSS [Fig. 2(a)]. The simulation confirmed that a faster tapering toward the end of the antenna can still provide an acceptable reflection coefficient ($|S_{11}| < -10$ dB) while minimizing the directivity. Furthermore, examining the simulated antenna patterns, we observed that the bandwidth can be extended to higher frequencies, but at the cost of patterns becoming conical toward the upper plane. It is suggested that one can optimize the slope of the antenna at the position corresponding to frequencies of interest to improve

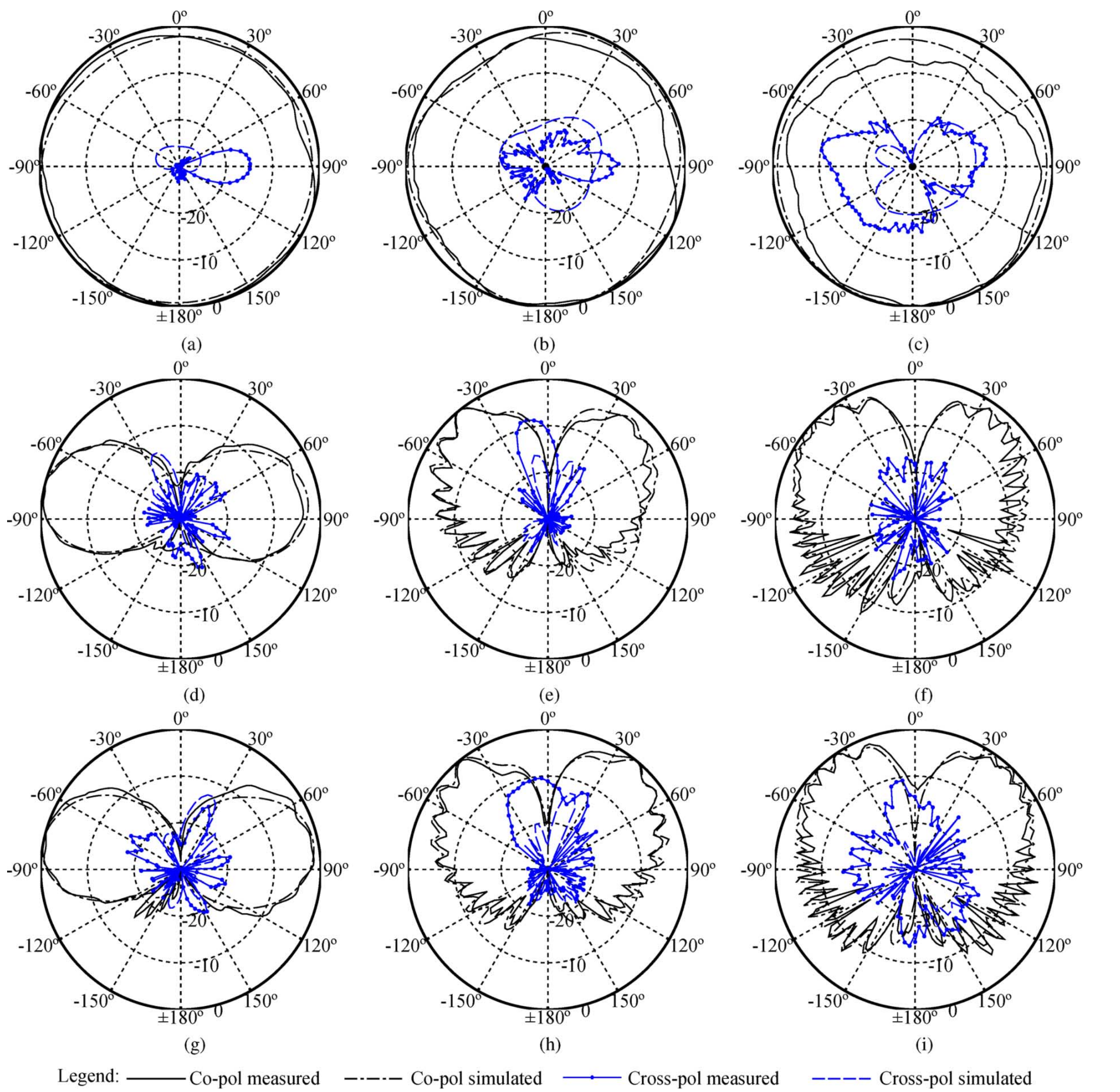

Fig. 5. Normalized simulated and measured radiation patterns for the via-wall antenna at $f = 7, 11.5$, and 16 GHz. (a) 7 GHz, xy-plane. (b) 11.5 GHz, xy-plane. (c) 16 GHz, xy-plane. (d) 7 GHz, xz-plane. (e) 11.5 GHz, xz-plane. (f) 16 GHz, xz-plane. (g) 7 GHz, yz-plane. (h) 11.5 GHz, yz-plane. (i) 16 GHz, yz-plane.

the pattern quality while keeping $|S_{11}|$ within the acceptable range.

The practical design starts by choosing W_2 and W_4 as the widths of HMSIWs exhibiting cutoff frequencies at the desired lowest and highest operation frequencies, i.e., $W_{2,4} = c/(4\sqrt{\varepsilon_r} f_{\min,\max})$. Furthermore, as an empirical rule of thumb, we suggest selecting a starting value of $W_5 = W_4/2$, and W_3 slightly larger than W_4. Afterwards, the lengths L_i can be optimized for minimal directivity while keeping $|S_{11}|$ below -10 dB.

For an equivalent antenna employing via holes as metallic wall, the effective width formula [9] is used to calculate the widths of the via-wall antenna at all relevant positions W_1 to W_5 [Fig. 2(a) and (b)]. This provides a good estimation as the relationship between w and w_{eff} can be linearly approximated due to the small variation of the width along the antenna. Simulations also show nearly identical behaviors of the designed PEC wall and real via-wall antenna.

C. Manufacture

The antenna with via sidewalls is fabricated with copper rivets of diameter $d = 1.05$ mm and spacing of $s = 1.6$ mm. For the transition, first a larger hole is drilled to accomodate the coaxial transition [Fig. 2(a)]. At this position, a copper pad is soldered to the bottom of the substrate [Fig. 2(c)]. The capacitive gap made of Rogers TMM10 with the copper removed from the upper side is then inserted at the bottom of the transition, and the SMA coaxial connector consisting of a metallic probe surrounded by a Teflon isolator is soldered at the top of the substrate. All air gaps should be avoided for lowest reflections at the transition. This manufacture process was found to be convenient and robust.

IV. Simulated and Experimental Results

This section demonstrates and compares the simulation and experimental results of the antenna bandwidth and radiation characteristics.

A. Reflection Coefficient and Bandwidth

Fig. 4 shows the correspondence between simulation and measurement for the via-wall antenna. The antenna demonstrates a very large bandwidth of $\mathrm{BW} = 16 : 6.7 \approx 2.4 : 1$ for $|S_{11}| < -10$ dB. The lowest operation frequency of 6.7 GHz is mainly controlled by the feeding structure's dimensions—more specifically, the parameters W_1, W_2, L_1, and l_t—whereas the highest frequency of operation is set by the progressive tapering of the antenna provided it is within the frequency range given by the feed.

B. Radiation Pattern

The radiation patterns in the xy-, xz-, and yz-planes at three chosen frequencies are shown in Fig. 5. At 7 GHz, the pattern resembles that of a small magnetic dipole. This is reasonable as the antenna only radiates for a short part of the open side of HMSIW. At higher frequencies, the radiation pattern becomes slightly conical in the upper plane $(z > 0)$, and some ripples appear. This can be explained as follows: Before the wave reaches the position at which the operating frequency becomes cutoff frequency, a very small part of the energy is radiated as it is guided along the HMSIW aperture. The higher the frequency, the longer the wave travels along the HMSIW, and the more ripples are generated in the pattern. However, most of the power still radiates around the cutoff frequency position, so the level of the ripples remains within an reasonable range [< 5 dB at $f = 11.5$ GHz and < 3 dB at $f = 16$ GHz shown in Fig. 5(e), (h), (f), and (i)]. An analogy for that is a long magnetic dipole with nonuniform current distribution, i.e., starting with low current magnitude and ending with much larger magnitude over a short portion. Another possible reason is that the reflected wave also creates a standing wave that contributes to the ripples. It is also worth mentioning that the amplitude of the ripples becomes smaller as frequency increases.

The omnidirectional broadside pattern can be observed in the xy-plane transverse to the HMSIW axis at low frequencies [Fig. 5(a) and (b)]. As the operating frequency increases, the pattern becomes slightly conical with a maximum in the upper plane. Therefore, the pattern for xy-plane $(\theta = 90^\circ)$ becomes less nondirectional [Fig. 5(c)]. However, HFSS simulations show that the pattern is still nondirectional at angle θ around the peak gain depending on operating frequency. This can also be partly observed from the patterns for xz- and yz-planes [Fig. 5(f) and (i)].

Fig. 6 shows the realized maximum gain and directivity of the antenna. The simulated antenna directivity is less than 7 dB for the whole bandwidth and less than 6 dB above 14 GHz due to the faster tapering. Simulated results show only 1 dB difference between the realized gain and directivity, which means about 80% of efficiency for the whole bandwidth. The measured gain is in acceptable agreement with the simulated realized gain in most of the operating bandwidth, with slight deviations that can

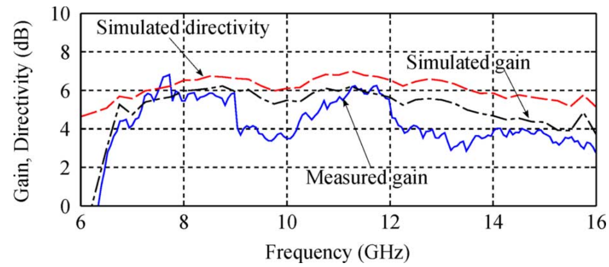

Fig. 6. Simulated and measured realized maximum gains compared with maximum directivity.

be explained by uncertainties in the reference data for the absolute gain measurements and the fact that the peak gain is only measured along the three principal Cartesian planes.

V. Conclusion

A traveling-wave HMSIW antenna has been proposed in this letter. The HMSIW changes from guided mode to radiation mode along its propagation axis by tapering its width to progressively increase its cutoff frequency along its length. While maintaining the advantages of HMSIW structure such as large power-handling capability, small transverse size, low profile, low cost, and easy fabrication, the antenna attains very wide bandwidth with omnidirectional pattern and horizontal polarization. The HMSIW antenna is long in terms of wavelength, but thin and planar, and could be easily integrated into metallic structures, such as poles or airplane fuselages. The scaling for mm-wave applications appears also promising, e.g., for integration into sides of portable devices.

Using the presented principle, the shape of the antenna can be optimized to enhance the antenna performance and reduce the size, or it can be tailored for specific applications, e.g., achieving a narrow bandwidth with a short-dipole-like pattern.

References

[1] W. Hong, B. Liu, Y. Wang, Q. Lai, H. Tang, X. X. Yin, Y. D. Dong, Y. Zhang, and K. Wu, "Half mode substrate integrated waveguide: A new guided wave structure for microwave and millimeter wave application," in *Proc. Joint 31st Int. Infr. Millim. Waves Conf./14th Int. Teraherz Electron. Conf. (IRMMW-THz)*, Sep. 2006, p. 219.

[2] D. Deslandes and K. Wu, "Integrated microstrip and rectangular waveguide in planar form," *IEEE Microw. Wireless Compon. Lett.*, vol. 11, no. 2, pp. 68–70, Feb. 2001.

[3] Q. Lai, C. Fumeaux, and W. Hong, "Periodic leaky-wave antennas fed by a modified half-mode substrate integrated waveguide," *Microw., Antennas Propag.*, vol. 6, no. 5, pp. 594–601, 2012.

[4] Q. H. Lai, W. Hong, Z. Q. Kuai, Y. S. Zhang, and K. Wu, "Half-mode substrate integrated waveguide transverse slot array antennas," *IEEE Trans. Antennas Propag.*, vol. 57, no. 4, pp. 1064–1072, Apr. 2009.

[5] J. Xu, W. Hong, H. Tang, Z. Kuai, and K. Wu, "Half-mode substrate integrated waveguide (HMSIW) leaky-wave antenna for millimeter-wave applications," *IEEE Antennas Wireless Propag. Lett.*, vol. 7, pp. 85–88, 2008.

[6] E. Arnieri, G. Amendola, L. Boccia, and G. Di Massa, "Coaxially fed substrate integrated radiating waveguides," in *Proc. IEEE Antennas Propag. Soc. Int. Symp.*, Jun. 2007, pp. 2718–2721.

[7] M. Clenet, J. Litzenberger, D. Lee, S. Thirakoune, G. Morin, and Y. Antar, "Laminated waveguide as radiating element for array applications," *IEEE Trans. Antennas Propag.*, vol. 54, no. 5, pp. 1481–1487, May 2006.

[8] Q. Lai, C. Fumeaux, W. Hong, and R. Vahldieck, "Characterization of the propagation properties of the half-mode substrate integrated waveguide," *IEEE Trans. Microw. Theory Tech.*, vol. 57, no. 8, pp. 1996–2004, Aug. 2009.

[9] F. Xu and K. Wu, "Guided-wave and leakage characteristics of substrate integrated waveguide," *IEEE Trans. Microw. Theory Tech.*, vol. 53, no. 1, pp. 66–73, Jan. 2005.